Some aspects of Compton polarimetry for the ILC at the low beam energy around 5 GeV

Gideon Alexander^{a,c} and Pavel Starovoitov^{b,c}

^{a}Physics Department, Tel-Aviv University, Tel-Aviv, Israel
^{b}National Center for Particle and High Energy Physics, Minsk, Belarus
^{c}DESY Zeuthen, Zeuthen, Germany

1 Introduction

Among the options for the polarimetry of the positron beam near its production region in the International Linear Collider (ILC) we consider here the Compton polarimeter which has been used previously in several electron-positron colliders at their interaction point. Here we study in some details the option of a Compton polarimeter positioned after the ILC Damping Ring (DR) which is expected to be operated at 5 GeV. In particular we present estimates for the γe luminosity, the rate of Compton events and their properties and the precision attainable for an asymmetry measurement.

1.1 General remarks

A priori there are several methods that can be adopted for Compton polarimetry, among them, one can choose between the detection of the final state photon or the final state electron[1] or one can choose to detect them in coincidence. Furthermore when adopting to detect e.g. the photon final state, one does distinguish between the method known as the Multi-Photon mode and the Single-Photon mode. As for the laser system one may consider the continuous laser mode or a pulsed laser configuration.

A comprehensive study of a proposed Compton polarimeter for the e^+e^- TESLA collider at the Interaction Point (IP) region, where many of the above mentioned variations are discussed, is given in Ref. [1] for the linear collider beam energies of 45.6, 250 and 400 GeV. The work discussed here is based in part on that thorough work.

---

[1]Whenever an electron is mentioned it also means a positron.

2 The γe Luminosity

2.1 Luminosity for continuous lasers

The luminosity $\mathcal{L}$ of a continuous laser colliding with a round pulsed electron beam, that is $\sigma_x = \sigma_y = \sigma$, can be expressed [2,3] as:

$$\mathcal{L} = \frac{1 + \cos\theta_0}{\sqrt{2\pi}} \frac{I_e}{e} \frac{P_L \lambda}{hc^2} \frac{1}{\sqrt{\sigma_e^2 + \sigma_\gamma^2}} \frac{1}{\sin\theta_0}, \tag{1}$$

where θ_0 is the crossing angle of the two beams, I_e is the mean electron current, P_L is the power of the laser, λ is the wavelength of the laser and σ_e and σ_γ are the rms beam sizes. As expected the luminosity will decrease substantially when the angle between the laser and the beam will approach 90° as seen in Fig. 1 so that a continuous laser beam perpendicular to the electron beam will result in an undesired low luminosity[2].
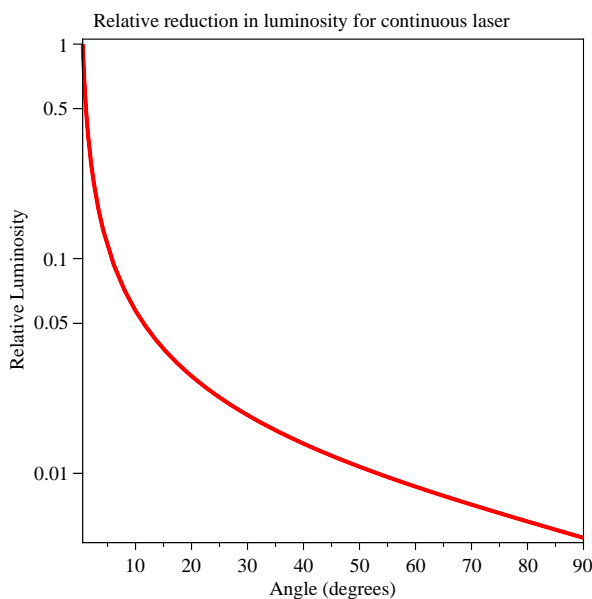

Figure 1: The relative luminosity as a function of the crossing angle θ_0 of incident electron and laser beams.

For small crossing angle θ_0 one has:

$$\mathcal{L} = 8.36 \ 10^{24} cm^{-2} s^{-1} \frac{\lambda}{\sqrt{\sigma_e^2 + \sigma_\gamma^2}} \frac{I_e(\mu A) P_L(W)}{\theta_0(rad)} \ . \tag{2}$$

According to Ref. [1] at TESLA, where $\sigma_e \ll \sigma_\gamma$, and with the following parameters settings:

---

[2]Note that $\theta_0 = 0^o$ means here that the laser and the beam directions are exactly opposite.

2

$\theta_0 = 0.01$ rad,
$\lambda = 1.064\ \mu$m $= 1.165$ eV,
$\sigma_\gamma = 50\ \mu$m,
$P_L = 1.0$ W,
$I_e = 45\ \mu$A,
one obtains a luminosity of

$$\mathcal{L}(TESLA) \ = \ 0.80 \times 10^{27}\ cm^{-2}s^{-1}\ . \tag{3}$$

According to the current design of the ILC the specifications of the DR are [4]:

injected normalized (x,y) emittance:	0.01 m
extracted normalized horizontal emittance:	8 μm
extracted normalized vertical emittance:	0.02 μm
positron energy:	5000 MeV

Assuming a beta of 20m we find after the DR:

a horizontal beam size of:	130 μm
a vertical beam size of:	6.5 μm.

The corresponding positron beam size before the DR is estimated to be ~ 4.5 mm.

To evaluate the luminosity before and after the DR it is useful to consult Ref. [5]. Since the area of the electron beam after the DR is much smaller than that of the laser beam the condition that $\sigma_e \ll \sigma_\gamma$ is satisfied so that luminosity calculation via Eqs. 2 and 3 should be approximately correct although the shape of the electron beam is evidently far from being circular. In Ref. [1] a laser of energy of 1.165 eV was chosen for the TESLA IP Compton polarimeter. At a positron beam energy of 5 GeV it is however advantageous to use a higher laser photon energy, for a example 4.66 eV (266 nm), to achieve a better asymmetry analyzing power (see Fig. 2).

Inasmuch that the other parameters, apart from the laser energy, remain the same as those listed in Ref. [1] for the IP position, the luminosity after the DR will be reduced by a factor 4 namely:

$$\mathcal{L}(ILC\ at\ 5\ GeV\ after\ the\ DR) \ \simeq 0.20 \times 10^{27}\ cm^{-2}s^{-1}\ . \tag{4}$$

Taking the positron beam before the DR to be of a circular form with a radius of 4.5/2 mm, the expected luminosity is:

$$\mathcal{L}(ILC\ at\ 5\ GeV\ before\ the\ DR) \ \simeq 0.44 \times 10^{25}\ cm^{-2}s^{-1} \tag{5}$$

that is about a factor 45 times less than obtained after the DR. This is mainly due to the small effective overlap of beams (4.5mm electron beam with 50 μm laser spot) since it's quite an effort to provide 1 W of laser light power over all the electron beam spot. This condition before the DR maybe solved, for example, by the use of a Bhabha-based polarimeter [10].

2.2 Luminosity values with pulsed lasers

For a pulsed laser the γe luminosity is given by [5]:

$$\mathcal{L} = f_b N_e N_\gamma g \qquad (6)$$

where f_b is the number of bunch crossing per second, N_e number of electrons per bunch, N_γ number of photons per laser pulse and g is a geometrical factor which takes in account the spatial overlap of the two beams. For a small crossing angle θ_0 one has:

$$g^{-1} = 2\pi \sqrt{\sigma_{xe}^2 + \sigma_{x\gamma}^2} \sqrt{(\sigma_{ye}^2 + \sigma_{y\gamma}^2)cos^2(\theta_0/2) + (\sigma_{ze}^2 + \sigma_{z\gamma}^2)sin^2(\theta_0/2)} \qquad (7)$$

where a vertical beam crossing is assumed. If the transverse dimensions of the electron beam are small in comparison to the laser focus i.e., $\sigma_{xe} \ll \sigma_{x\gamma}$ and $\sigma_{ye} \ll \sigma_{y\gamma}$ (which certainly is valid at the IP region but not necessarily after the DR), one obtains for g^{-1} :

$$g^{-1} = 2\pi\sigma_{x\gamma}\sigma_{y\gamma}\sqrt{1 + (0.5\theta_0\sigma_{z\gamma}/\sigma_{y\gamma})^2} \qquad (8)$$

and for the luminosity:

$$\mathcal{L} = \frac{f_b N_e N_\gamma}{2\pi\sigma_{x\gamma}\sigma_{y\gamma}\sqrt{1 + (0.5\theta_0\sigma_{z\gamma}/\sigma_{y\gamma})^2}} = \frac{\mathcal{L}_{max}}{\sqrt{1 + (0.5\theta_0\sigma_{z\gamma}/\sigma_{y\gamma})^2}} \qquad (9)$$

where $\mathcal{L}_{max}$ is the maximum luminosity reached at very small θ_0 for a given transverse size $\sigma_{x\gamma}\sigma_{y\gamma}$, namely:

$$\mathcal{L}_{max} = \frac{f_b N_e N_\gamma}{2\pi\sigma_{x\gamma}\sigma_{y\gamma}} \ . \qquad (10)$$

Note that this last formula is very similar to the expression given for the luminosity of e^+e^- colliding beams.

The luminosity values and their variations in the pulsed laser operation mode at the IP of TESLA are dealt with in Ref. [1] where the dimensions of the electron bunches are smaller than that of the laser. These luminosity values can be utilized for our luminosity estimations as long as all the ILC parameters are the same as TESLA apart from the electron bunch dimensions which after the DR are obviously different. To this end it is sufficient to evaluate, with the help of Eq. 7, the change in the geometrical factor g when moving from the IP to the region after the DR. Now the ratio $g(DR)/g(IP)$ for very small θ_0 and with the condition that $\sigma_{xe}(IP) \ll \sigma_{x\gamma}$ and $\sigma_{ye}(IP) \ll \sigma_{y\gamma}$, is equal to:

$$R \approx \frac{g(DR)}{g(IP)} = \frac{\sigma_{x\gamma}\sigma_{y\gamma}}{\sqrt{(\sigma_{xe}^2(DR) + \sigma_{x\gamma}^2)(\sigma_{ye}^2(DR) + \sigma_{y\gamma}^2)}} \ . \qquad (11)$$

Using the value given in [1] of $\sigma_{x\gamma} = \sigma_{x\gamma} = 50\mu$m and for the beam dimensions after the DR of $\sigma_{xe}(DR) = 130\mu$m and $\sigma_{ye}(DR) = 6.5\mu$m, one obtains R=0.356. At the position before the

DR the value is very small indeed and equal to R=0.00012. Thus the luminosity values after the DR (at 5 GeV) are roughly 35% of those given in the configuration discussed in [1] at the TESLA IP. For example at TESLA-500 with $f_b = 14100$ bunches per second and $N_e = 2 \times 10^{10}$ electrons per bunch one gets at the IP:

$$\mathcal{L}_{max}(IP) \;=\; 4.49 \times 10^{13} \frac{N_\gamma}{\sigma_{x\gamma}\sigma_{y\gamma}[cm^2]} \; cm^{-2}s^{-1} \tag{12}$$

where N_γ is the number of laser photons per pulse and the laser is fired with the same pulse repetition rate as the accelerator. The γe luminosities that can be achieved at 5 GeV, after the DR, with a pulsed laser Compton polarimeter are dealt with in section 3.2.

3   The Compton scattering cross section

The event rate of the polarimeter can be evaluated via the relation $N_{events} \;=\; \mathcal{L} \times \sigma_C$ where $\sigma_C \equiv \sigma_{Compton}$. The cross section value to be applied depends of course on the specific polarimeter set up e.g., on the angular acceptance of the outgoing photons (positrons). In reference [6–8], the Compton differential cross section of polarized, transverse and/or longitudinal, electron and circular or linear photon, is given. In evaluating the expected event rate of a polarimeter it may therefore be more convenient at times to use for the Compton scattering one of the formulae defined in the Lab system which are presented in the following subsection.
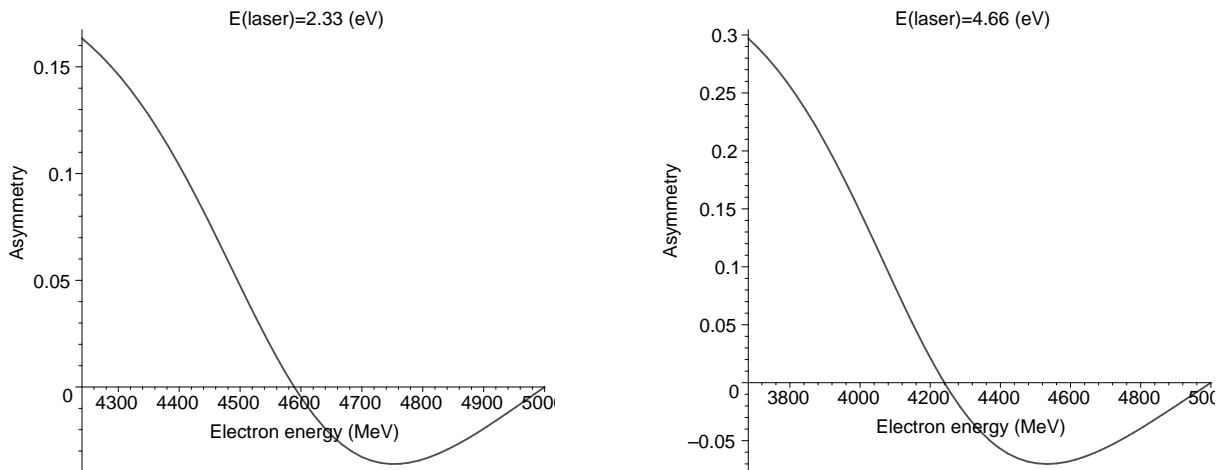

Figure 2: The asymmetry, defined in Eq. 19, as a function of the final state electron energy for incident beam energy of 5000 MeV and laser energies of 2.33 eV (left figure) and 4.66 eV (right figure).

3.1 The Compton differential cross section

In the present work, as frequently is done, we use the dimensionless variables x, y and r which are defined as:

$$x = \frac{4E_0\omega_0}{m^2}cos^2(\theta_0/2) \simeq \frac{4E_0\omega_0}{m^2} \tag{13}$$

$$y = 1 - \frac{E}{E_0} = \frac{\omega}{E_0} \quad \text{and} \quad r = \frac{y}{x(1-y)} \tag{14}$$

where:

E_0 and E are the initial and final electron energies,

ω_0 and ω are the initial and final photon energies,

m is the mass of the electron,

θ_0 is the crossing angle between the electron beam and the laser.

The spin dependent differential cross section with respect to the final state normalised photon energy y is given by:

$$\frac{d\sigma}{dy} = \frac{2\sigma_0}{x}\left[\frac{1}{1-y} + 1 - y - 4r(1-r) + P\lambda rx(1-2r)(2-y)\right] \tag{15}$$

where $\sigma_0 = \pi r_0^2 = 0.2495$ barn, P is the initial electron helicity ($P = \pm 1$) and λ is the initial photon helicity ($\lambda = \pm 1$).

At times it is more convenient to use the Compton differential cross section $d\sigma/d\omega$, rather than $d\sigma/dy$, which also is defined in the Lab system. In this case one may use e.g. a formula for $d\sigma/d\omega$, for an unpolarised beam which is given by [9]:

$$\frac{d\sigma}{d\omega} = \frac{\pi r_0^2}{2}\frac{m^2}{\omega_0 E_0^2}\left[\frac{m^4}{4\omega_0^2 E_0^2}\left(\frac{\omega}{E_0-\omega}\right)^2 - \frac{m^2}{\omega_0 E_0}\frac{\omega}{E_0-\omega} + \frac{E_0-\omega}{E_0} + \frac{E_0}{E_0-\omega}\right] . \tag{16}$$

The energy spectra of the final state electron and photons are image mirrors and are continuous up to the so called Compton edge so that one has:

$$\omega_{max} = E_0\frac{x}{1+x}; \qquad E_{min} = E_0\frac{1}{1+x} . \tag{17}$$

Using the parameters x and y, the scattered electron and photon angles are given by:

$$\theta_\gamma = \frac{m}{E_0}\sqrt{\frac{x}{y} - (x+1)}; \qquad \theta_e = \frac{y}{1-y}\theta_\gamma . \tag{18}$$

The predicted asymmetry between $P = -1$ and $P = +1$ polarization states is defined by

$$Asy = \frac{d\sigma(P=-1)/dy - d\sigma(P=+1)/dy}{d\sigma(P=-1)/dy + d\sigma(P=+1)/dy} . \tag{19}$$
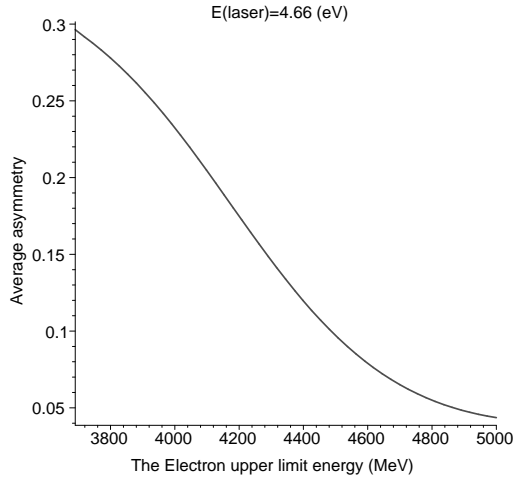
6

Figure 3: The asymmetry value averaged over the lowest kinematically allowed outgoing electron energy of 3681 MeV to the energy value indicated on the x-axis for Compton scattering of 5000 MeV electrons with a laser beam of 4.66 MeV both defined in the Lab system.

The behavior of this asymmetry for a 5000 MeV beam as a function of the outgoing electron energy is shown in Fig. 2 for the two laser energies of 2.33 and 4.66 eV. For a Compton scattering of 5000 MeV electrons on a laser beam of 4.66 eV, the asymmetry value, averaged over the outgoing electron energy from its lowest kinematically allowed value of 3681 MeV to its value indicated by the x-axis, is shown in Fig. 3.

In Table 1 are given the total Compton cross section values which were obtained by integrating Eq. 15 from $\omega=0$ to ω_{max} and setting $P = 0$.

Table 1: Kinematic parameters for three laser energies at E_0=5000 MeV and the total Compton cross section for unpolarised beams. The luminosity and maximum event rates are calculated for a continuous laser and a polarimeter situated after the DR and for the case where $\theta_0 = 0.01$, $\sigma_\gamma = 50\mu$m, P_L=1 W and $I_e = 45\mu A$.

E_0 (MeV)	λ (nm)	ω_0 (eV)	x	ω_{max} (MeV)	E_{min} (MeV)	σ_{tot} (mb)	$\mathcal{L}$umi $(10^{27}cm^{-2}s^{-1})$	Max. rate $(\sec^{-1})$
5000	1064	1.66	0.090	411.1	4588.9	612.0	0.8	490
"	532	2.33	0.179	759.7	4240.3	568.7	0.4	227
"	266	4.66	0.358	1319.0	3681.0	502.8	0.2	101

In practice in a polarimeter there exists a lower limit on the final state photon energy that is measured. As a consequence, the actual value of the used cross section is smaller than that

7

listed in Table 1. To evaluate the fraction of the useful cross section we plot in Fig. 4 the value for integrated differential Compton scattering in the limits from ω given by the x-axis to ω_{max}. The figures are for electron beams of 5000 MeV and a laser of 2.33 eV (left figure) and 4.66 eV (right figure).
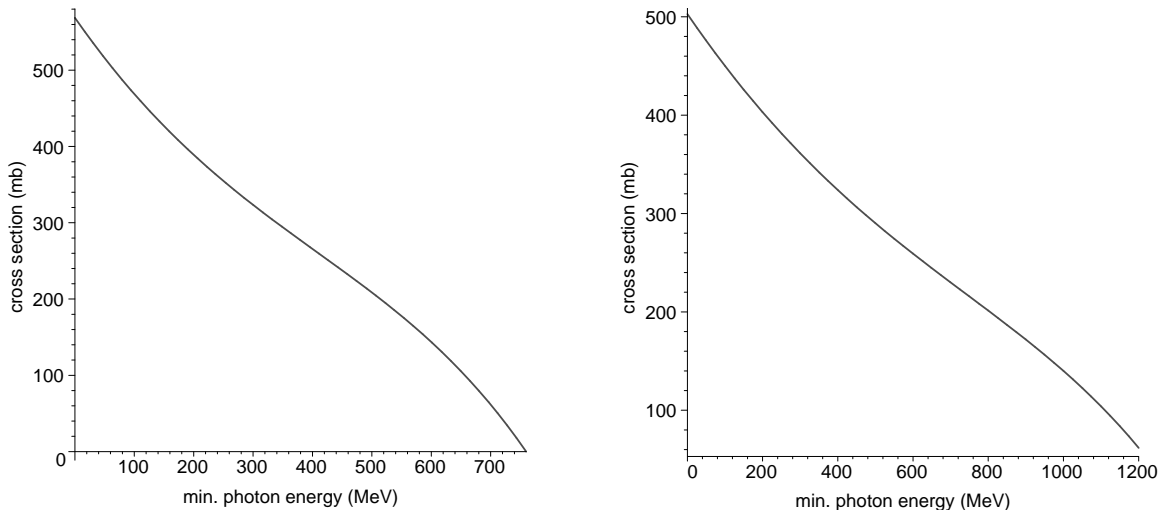

Figure 4: The integrated differential Compton scattering cross section between ω (given on the x-axis) and ω_{max}. The y-axis represents σ in mb. Left: E_0=5000 MeV and ω_0=2.33 eV. Right: E_0=5000 MeV and ω_0=4.66 eV.

3.2 Compton scattering event rate

For the estimation of the Compton scattering luminosity and event rate, shown in Table 1, we consider a polarimeter using a continuous laser placed in the position after the DR and applying the same parameters as used in Ref. [1] namely: $\theta_0 = 0$, $\sigma_\gamma = 50\mu$m, P_L=1 W and $I_e = 45\mu A$. In the same Table are also listed the numbers of Compton scattering events which are deduced from the total cross sections obtained from integrating $d\sigma/d\omega$ between ω=0 to ω_{max}. However as discussed above, the actual Compton scattering rate detected by the polarimeter will be just a little bit smaller due to energy cuts since majority of photons (see cross section (15)) will go in the direction of initial electron beam. One will need either large distance from Compton IP to detector or really high granularity detector operated in Single-Photon mode in order to distinguish between photons with different energies. It can be evaluated with the help of Fig. 4.

In Table 2 are presented the expected γe luminosities for several pulsed lasers with a repetition rate of 5 Hz of the types which are offered by several commercial companies (see e.g. Fig. 5). it is to note from this Table that for a pulse duration of 8 ns the γe luminosities are already higher by 5 order of magnitude than those obtained by a continuous laser. Shortening the pulse

duration to 1 ns an additional factor of 10 is gained for the luminosity. For completeness we show in Table 3 the expected luminosities from the Nd:YAG lasers with repetition rate of 3MHz which are proposed to be used in connection with ILC such as measuring the beam energy.

Table 2: The luminosities expected from pulsed lasers impinging on beams of the ILC at 5 GeV. The lasers are Nd:YAG with a repetition rate of 5Hz.

ω_0 (eV)	λ (nm)	Energy (mJ)	Pulse (ns)	$\mathcal{L}$umi $(cm^{-2}s^{-1})$	Pulse (ns)	$\mathcal{L}$umi $(cm^{-2}s^{-1})$	Pulse (ps)	$\mathcal{L}$umi $(cm^{-2}s^{-1})$
1.66	1064	700	8	1.7×10^{33}	1	1.4×10^{34}	10	2.0×10^{35}
2.33	532	300	8	3.7×10^{32}	1	2.9×10^{33}	10	4.3×10^{34}
4.66	266	60	8	3.7×10^{31}	1	2.9×10^{32}	10	4.3×10^{33}

Table 3: The luminosities expected from pulsed lasers, proposed for several tasks in the ILC, impinging on the accelerator beam at the energy of 5 GeV. The lasers type is Nd:YAG with a repetition rate of 3MHz.

ω_0 (eV)	λ (nm)	Energy (μJ)	Pulse (ps)	$\mathcal{L}$umi $(cm^{-2}s^{-1})$
1.66	1064	10	10	1.4×10^{31}
2.33	532	10	10	7.2×10^{30}
4.66	266	10	10	3.6×10^{30}

4   The asymmetry measurement

In the Compton longitudinal polarimetry there are in principle four different measurement methods that can be adopted. In two of them one measures and detects the outgoing photons, in a single mode or in multi-photon mode. In the two other modes one detects the single outgoing electron or a multi-bunch electrons. In the particular case dealt here, the outgoing electrons are of high energies, not far from the beam energy, and therefore their extraction from the accelerator pipe without disturbing the beam is tricky. The detection of the outgoing photons on the other hand is simpler. To this end however the beam has to be deflected to let the photons go out of the pipe after which the beam has to be deflected back. This procedure is expected not to disturb the polarization level of the beam.

The spin asymmetry, or analyzing power, is defined as:

$$A = \frac{\sigma^- - \sigma^+}{\sigma^- + \sigma^+} \qquad (20)$$

where the $(-)$ and $(+)$ denote opposite and like sign helicity configurations of the two beams with $P\lambda = \pm 1$. The opposite sign helicity configuration $(P\lambda = -1)$, which has parallel spins $(m_j = 3/2)$, dominates at the Compton edge over the other helicity and spin orientation $(P\lambda = +1$ and $m_j = 1/2)$. The asymmetry we define here, is therefore positive at the Compton edge.

In general the advantages and disadvantages of the single-photon and multi-photon modes can be summarized as follows:

Single-photon mode advantages are:
   1. Can choose large asymmetry;
   2. Easy comparison with $d\sigma/d\omega$;
The disadvantages are:
   1. Needs long time to achieve, say a precision of $\Delta P/P = .01$;
   2. Detector is more complex;
Multi-photon mode advantages are:
   1. Essentially independent of Bremsstrahlung background and detector cutoff energy;
   2. Needs much shorter time to arrive to say $dP/P = .01$;
The disadvantage is:
   1. No easy monitoring of calorimeter performance.

For Compton operation in the multi-photon mode it is convenient to define a multi-photon asymmetry or analyzing power as

$$A_p = \frac{I^- - I^+}{I^- + I^+} , \qquad (21)$$

where I^+ and I^- are the total photon energies deposited in the detector for helicity state $P\lambda = +1$ and $P\lambda = -1$ of initial γe system (cf Eq. 15), namely:

$$I^\pm = \int y \frac{d\sigma^\pm}{dy} dy. \qquad (22)$$

Clearly the value of A_p depends on the range of integration which inasmuch that it cannot be controlled experimentally, yield a relatively low value of the asymmetry since the asymmetry changes sign when moving from the lowest photon energy to its maximal value. In the multi-photon mode one uses a calorimeter which measures the total energy deposited by the photons.

It is also useful to calculate the average energy of the outgoing photons, $\bar{\omega}$, which is given by

$$\bar{\omega} = \frac{E_0 \int \frac{d\sigma}{dy} y \, dy}{\int \frac{d\sigma}{dy} dy} \qquad (23)$$

From this we get for E_0=5 GeV, and ω_o=2.33 eV that

$$\bar{\omega}_0 = 374.95 \text{ MeV}, \ \bar{\omega}_- = 389.35 \text{ MeV and } \bar{\omega}_+ = 359.45 \text{ MeV}.$$

To note is that the desired asymmetry measurement is not given by $(\bar{\omega}_- - \bar{\omega}_+)/(\bar{\omega}_- + \bar{\omega}_+)$ however it allows us to calculate the integrated energy collected in a given time by the polarimeter calorimeter. From Table 1 we find that for 5 GeV electron beam and a laser of 2.33 eV, about 220 Compton photon are emitted over the entire polar and azimuthal angles. Thus for an unpolarised electron beam the energy absorbed by the detector is 220×375 MeV/sec. This energy deposition will be reduced substantially, e.g. by a factor 10 if the azimuthal acceptance is restricted to 36°.

Before calculating the error on the asymmetry it is instructive to express it in terms of the average photon energies, namely:

$$A_p \ = \ \frac{\bar{\omega}_- \int \frac{d\sigma_-}{dy} dy - \bar{\omega}_+ \int \frac{d\sigma_+}{dy} dy}{\bar{\omega}_- \int \frac{d\sigma_-}{dy} dy + \bar{\omega}_+ \int \frac{d\sigma_+}{dy} dy} \tag{24}$$

Again for our case of 5 GeV electron beam and a laser of 2.33 eV, we have:

$$\int \frac{d\sigma_-}{dy} dy = 2.94 \times 10^6 \ \text{ and } \ \int \frac{d\sigma_+}{dy} dy = 2.75 \times 10^6 \tag{25}$$

with the results that A_p=0.074, the same value obtained earlier from Eq. 21.

4.1 The asymmetry error

The intrinsic asymmetry error depends above all on operation mode and the precision of the electro-magnetic calorimeter chosen for the polarimeter. For the existing options out of which a calorimeter can be selected the reader is advised to consult for example Ref. [11]. Here we select a polarimeter calorimeter with an energy resolution of the form:

$$\frac{\sigma}{E} \ = \ \frac{10\%}{\sqrt{E(GeV)}} \ . \tag{26}$$

The absolute error on A_p is simply given by

$$\Delta A_p \ = \ \left| \frac{dA_p}{d\omega_-} \right| \Delta\bar{\omega}_- + \left| \frac{dA_p}{d\omega_+} \right| \Delta\bar{\omega}_+ \tag{27}$$

The relative precision which will be obtained for a continuous 1.165, 2.33 and 4.66 eV lasers as a function of the measuring time is shown in Fig. 5 assuming an efficiency of 100% and neglecting any possible background contribution. As can be seen, to achieve a relative asymmetry uncertainty of 5%, the needed time for the data collection is of the order of 10 seconds for a
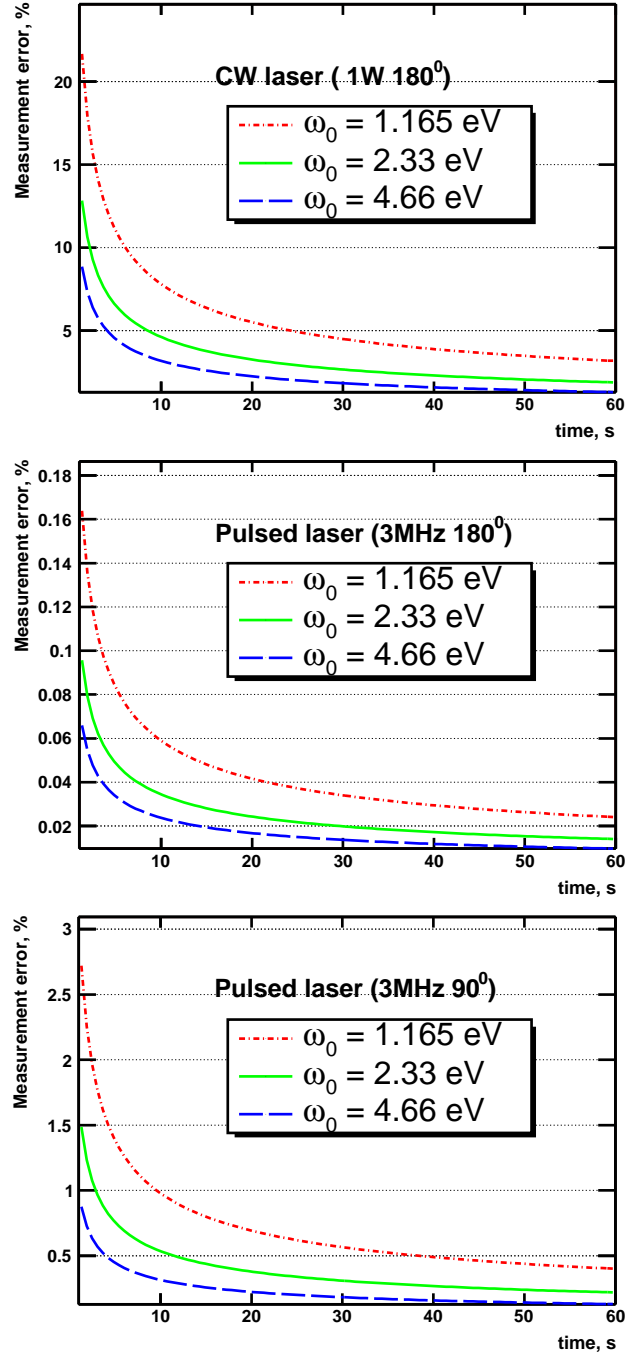
Figure 5: The asymmetry A_p relative error as a function of the measurement time for a 5 GeV electron beam and laser energies ω_0 of 1.165, 2.33 and 4.66 eV (see Tables 1 and 3). The upper figure corresponds to a continuous laser whereas the other two figures are for a pulsed laser with a repetition rate of 3MHz. In the middle and lower figures the laser is directed respectively at 180° and 90^0 with respect to the electron beam.

12

2.33 eV continuous laser, quite sufficient for feedback purposes. Much shorter times will be needed for polarimeters equipped with a pulsed laser with a repetition rate of 3MHz as shown in Fig. 5. Finally it should be stressed that the lowest over all attainable uncertainty of the polarisation measurement will be dominated by the systematic error which so far could not have been estimated here due to the lack of a realistic ILC polarimeter design and its operation study via a Monte Carlo simulation.

Acknowledgments

References

[1] V. Gharibyan, N. Meyners, K.P. Schüler, *The TESLA Compton polarimeter*, Linear collider Note, LC-DET-2001-047.

[2] G. Bardin, et al., *Compton polarimeter studies for TESLA*, DESY print, TESLA 97-03.

[3] D.P. Barber et al., *The HERA polarimeter and the first observation of electron spin polarization at HERA*, Nucl. Inst. Meth. A329 (1993) 79.

[4] J. Brau et al., *International Linear Collider reference design report*, SLAC report, SLAC-R-857, 2007.

[5] T. Suzuki, *General formulae of luminosity for various types of colliding beam machines*, KEK-76-3 (1976), *http://ccdb4fs.kek.jp/cgi-bin/img_index?197624003* .

[6] G. Alexander et al., *Polarization at LEP*, CERN yellow report CERN 88-06, (G. Alexander et al., Eds.), Vol 2, pp. 3−49.

[7] F. W. Lipps, H. A. Tolhoek *Polarization phenomena of electrons and photons. II*, Physica XX (1954) pp. 395–405

[8] I. F. Ginzburg *Colliding γe and $\gamma\gamma$ Beams Based on the Single Pass e^+e^- Accelerators. 2. Polarization Effects. Monochromatization Improvement.* Nucl. Inst. Meth. A219 (1984) 5.

[9] I.C. Hsu et al., *Energy measurement of relativistic electron beams by laser Compton scattering*, Phys. Rev. E54 (1996) 5657.

[10] G. Alexander, E. Reinherz-Aronis, *Measurement of low energy longitudinal polarised positron beams via a Bhabha polarimeter*, LC Note: LC-PHSM-2005-006, *hep-ex/0505001*; G. Alexander, N.M. Shumeiko, P.M. Starovoitov, J.G. Suarez, Nonlinear Phenomena in Complex Systems, 8:2 (2005) 180; R. Dollan, K. Laihem, A. Schälicke *Monte Carlo based studies of a polarized positron*

source for international linear collider (ILC), Nucl. Inst. Meth. A559 (2006) 185; A. Schälicke et al., *Study on low-energy positron polarimetry*, Prepared for EPAC 06, Edinburgh, Scotland, 26-30 June 2006, *http://www.slac.stanford.edu/spires/find/hep/www?irn=7246846*; R. Dollan et al., *Low Energy Positron Polarimetry for the ILC*, Proc. of the LCWS07, 2007 (in print).

[11] R. Wigmans, *Calorimetry*, Clarendon Press, 2000.